Emergence of spatiotemporal chaos driven by far-field breakup of spiral waves in the plankton ecological systems

Quan-Xing Liu,[1] Gui-Quan Sun,[1] Bai-Lian Li,[2] and Zhen Jin[1,*]

[1]*Department of Mathematics, North University of China, Taiyuan, Shan'xi 030051, People's Republic of China*

[2]*Ecological Complexity and Modeling Laboratory, Department of Botany and Plant Sciences, University of California, Riverside, CA 92521-0124, USA*

(Dated: February 1, 2008)

Alexander B. Medvinsky *et al* [A. B. Medvinsky, I. A. Tikhonova, R. R. Aliev, B.-L. Li, Z.-S. Lin, and H. Malchow, Phys. Rev. E **64**, 021915 (2001)] and Marcus R. Garvie *et al* [M. R. Garvie and C. Trenchea, SIAM J. Control. Optim. **46**, 775-791 (2007)] shown that the minimal spatially extended reaction-diffusion model of phytoplankton-zooplankton can exhibit both regular, chaotic behavior, and spatiotemporal patterns in a patchy environment. Based on that, the spatial plankton model is furtherly investigated by means of computer simulations and theoretical analysis in the present paper when its parameters would be expected in the case of mixed Turing-Hopf bifurcation region. Our results show that the spiral waves exist in that region and the spatiotemporal chaos emerge, which arise from the far-field breakup of the spiral waves over large ranges of diffusion coefficients of phytoplankton and zooplankton. Moreover, the spatiotemporal chaos arising from the far-field breakup of spiral waves does not gradually involve the whole space within that region. Our results are confirmed by means of computation spectra and nonlinear bifurcation of wave trains. Finally, we give some explanations about the spatially structured patterns from the community level.

PACS numbers: 87.23.Cc, 82.40.Ck, 82.40.Bj, 92.20.jm
Keywords: Spiral waves; Spatio-temporal pattern; Plankton dynamics; Reaction-diffusion system

I. INTRODUCTION

There is a growing interest in the spatial pattern dynamics of ecological systems [1, 2, 3, 4, 5, 6, 7, 8, 9, 10, 11, 12, 13]. However, many mechanisms of the spatiotemporal variability of natural plankton populations are not known yet. Pronounced physical patterns like thermoclines, upwelling, fronts and eddies often set the frame for the biological process. Measurements of the underwater light field are made with state-of-the-art instruments and used to calculate concentrations of phytoplankton biomass (as chlorophyll) as well as other forms of organic matter. Very high diffusion of the marine environment would prevent the formation of any stable patch spatial distribution with much longer life-time than the typical time of biodynamics. Meanwhile, in addition to very changeable transient spatial patterns, there also exist other spatial patterns in marine environment, much more stable spatial structure associated with ocean fronts, spatiotemporal chaos [10, 11, 14], cyclonic rings, and so called meddies [15]. In fact, it is significant to create the biological basis for understanding spatial patterns of plankton [16]. For instance, the impact of space on the persistence of enriched ecological systems was proved in laboratory experiments [17]. Recently, it has been shown both in laboratory experiments [18] and theoretically [14, 19, 20, 21] that the existence of a spatial structure makes a predator-prey system less prone to extinction. This is due to the temporal variations of the density of different sub-populations can become asynchronous and the events of local extinction can be compensated due to re-colonization from other sites in the space [22]. During a long period of time, all the spiral waves have been widely observed in diverse physical, chemical, and biological systems [23, 24, 25, 26]. However, a quite limited number of documents [11, 12, 27, 28, 29] concern the spiral wave pattern and its breakup in the ecological systems.

The investigation of transition from regular patterns to spatiotemporally chaotic dynamics in spatially extended systems remains a challenge in nonlinear science [14, 23, 30, 31]. In a nonlinear ecology system, the two most commonly seen patterns are spiral waves and turbulence (spatio-temporal chaos) for the level of the community [32]. It has been recently shown that spontaneous spatiatemoporal pattern formation is an instrinsic property of a predator-prey system [11, 14, 33, 34, 35, 36] and spatiotemporal structures play an important role in ecological systems. For example, spatially induced speciation prevents the extinction of the predator-prey models [11, 12, 37]. So far, plankton patchiness has been observed on a wide range of spatial temporal scales [38, 39]. There exist various, often heuristic explanations of the spatial patterns phenomenon for these systems. It should be noted that, although conclusive evidence of ecological chaos is still to be found, there is a growing number of indications of chaos in real ecosystems [40, 41, 42, 43].

Recently developed models show that spatial self-structuring in multispecies systems can meet both criteria and provide a rich substrate for community-level

*Corresponding author; Electronic address: jinzhn@263.net

section and a major transition in evolution. In present paper, the scenario in the spatially extended plankton ecological system is observed by means of the numerical simulation. The system has been demonstrated to exhibit regular or chaostic, depending on the initial conditions and the parameter values [10, 29]. We find that the far-field breakup of the spiral wave leads to complex spatiotemporal chaos (or a turbulentlike state) in the spatially extended plankton model (1). Our results show that regular spiral wave pattern shifts into spatiotemporal chaos pattern by modulating the diffusion coefficients of the species.

II. MODEL

In this paper we study the spatially extended nutrient-phytoplankton-zooplankton-fish reaction-diffusion system. Following Scheffer's minimal approach [44], which was originally formulated as a system of ordinary differential equation (ODEs) and later developed models [10, 11, 29, 45, 46], as a further investigation, we study a two-variable phytoplankton and zooplankton model on the level of the community to describe pattern formation with the diffusion. The dimensionless model is written as

$$\frac{\partial p}{\partial t} = rp(1-p) - \frac{ap}{1+bp}h + d_p\nabla^2 p, \tag{1a}$$

$$\frac{\partial h}{\partial t} = \frac{ap}{1+bp}h - mh - f\frac{nh^2}{n^2+h^2} + d_h\nabla^2 h, \tag{1b}$$

where the parameters are r, a, b, m, n, d_p, d_h, and f which refer to work in Refs. [10, 11]. The explanation of model (1) relates to the nutrient-phytoplankton-zooplankton-fish ecological system [see Refs. [10, 29, 44] for details]. The local dynamics are given by

$$g_1(p,h) = rp(1-p) - \frac{ap}{1+bp}h, \tag{2a}$$

$$g_2(p,h) = \frac{ap}{1+bp}h - mh - f\frac{nh^2}{n^2+h^2}. \tag{2b}$$

From the earlier results [45] about non-spatial system of model (1) by means of numerical bifurcation analysis show that the bifurcation and bistability can be found in the system (1) when the parameters are varied within a realistic range. For the fixed parameters (see the caption of Fig. 1 and 2), we can see that the f controls the distance from Hopf bifurcation. For larger f, there exists only one stable steady state. As f is decreased further, the homogeneous steady state undergoes a saddle node bifurcation (SN), that is $f_{SN} = 0.658$. In this case, a stable and an unstable steady state become existence. Moreover, the bistability will emerge when the parameter f lies the interval $f_{SN} > f > f_c = 0.445$ (this value is more than the Hopf onset, $f_H = 0.3397$). There are three steady states: with these kinetics A and C are linearly stable while B is unstable. Outside this interval, the system (1) has unique nontrivial equilibrium. Recent studies [11, 29] shown that the systems (1) can well-develop the spiral waves in the oscillation regime, but where the authors only consider the special case, i.e., $d_p = d_h$. A few important issue have not yet been properly addressed such as the spatial pattern if $d_p \neq d_h$.

Here we report the result that emergence of spatiotemporal chaos due to breakup in the system under the $d_h \neq d_p$ case. We may now use the f and diffusion ratio, $\nu = d_h/d_p$, as control parameters to evaluate the region for the spiral wave. Turing instability in reaction-diffusion can be recast in terms of matrix stability [47, 48]. Such with the help of Maple software assistance algebra computing, we obtain the parameters space (f, ν) bifurcation diagrams of the spiral waves as showing Fig. 2, in which two lines are plotted, Hopf line (solid) and Turing lines (dotted) respectively. In domain I, located above all three bifurcation lines, the homogeneous steady states is the only stable solution of the system. Domain II are regions of homogeneous oscillation in two dimensional spaces [49]. In domain III, both Hopf and Turing instabilities occur, (i.e., mixed Turing-Hopf modes arise), in which the system generally produces the phase waves. Our results show that the system has spiral wave in this regions. One can see that a Hopf bifurcation can occur at the steady when the parameter f passes through a critical values f_H while the diffusion coefficients $d_p = d_h = 0$ and the bifurcation periodic solutions are stable. From our analysis (see Fig. 2), one could also see that the diffusion can induce Turing type instability for the spatial homogeneous stable periodic solutions and the spatially extended model (1) exhibit spatio-temporal chaos patterns. These spatial pattern formation arise from interaction between Hopf and Turing modes, and their subharmonics near hte codimension-two Hopf-Turing bifucation point. Special, it is interesting that spiral wave and travelling wave will appear when the parameters correspond to the Turing-Hopf bifurcation region III in the spatially extended model (1), i.e., the Turing instability and Hopf bifurcation occur simultaneously.

III. NUMERICAL RESULTS

The simulation is done in a two-dimensional (2D) Cartesian coordinate system with a grid size of 600×600. The fourth order Runger-Kutta integrating method is applied with a time step $\Delta t = 0.005$ time unit and a space step $\Delta x = \Delta y = 0.20$ length unit. The results remain the same when the reaction-diffusion equations were solved numerically in one and two spatial dimensions using a finite-difference approximation for the spatial derivatives and an explicit Euler method for the time integration. Neumann (zero-flux) boundary conditions

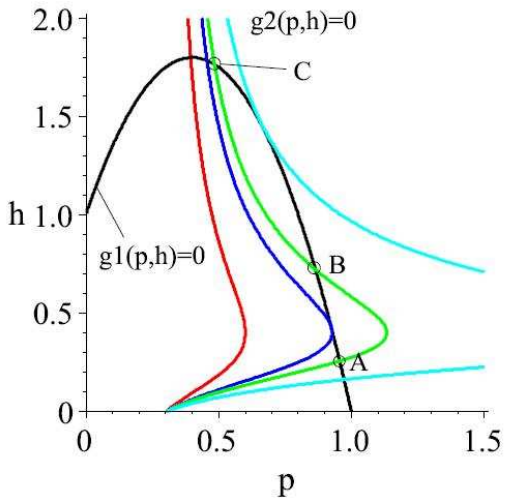

FIG. 1: The sketch map for the bistability and the Hopf bifurcation in the system (2) with $r = 5.0$, $a = 5.0$, $b = 5.0$, $m = 0.6$, and $n = 0.4$. The black curve is the $g_1(p, h)$. The colored curves are $g_2(p, h)$ with different values of f. The red curve: $f = 0.3$; the blue: $f = 0.445$; the green: $f = 0.5$; and the cyan: $f = 0.658$.

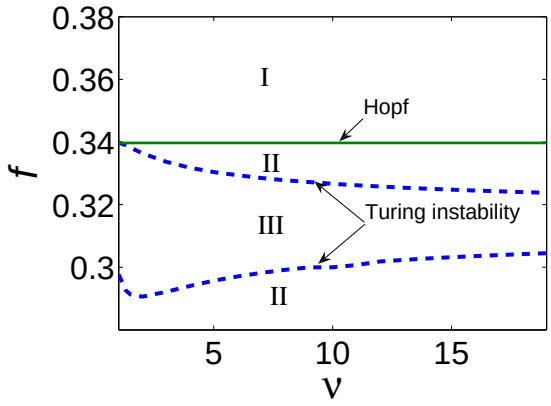

FIG. 2: The sketch map of parameter space (f, ν) bifurcation diagrams for the spatially extended system (1) with $r = 5.0$, $a = 5.0$, $b = 5.0$, $m = 0.6$, $d_p = 0.05$, and $n = 0.4$.

were emmployed in our simulation. The diffusion terms in Eqs. (1a) and (1b) often describe the spatial mixing of species due to self-motion of the organism. The typical diffusion coefficient of plankton patterns d_p is about 0.05, based on the parameters estimatie of Refs [50, 51] using the relationship between turbulent diffusion and the scale of the space in the sea. In the previous studies [10, 11, 29, 45, 46], the authors provided a valueable insight into the role of spatial pattern for the system (1) if $d_p = d_h$. From the biological meaning, the diffusion coefficients should satisfy $d_h \geq d_p$. However, in nature waters it is turbulent diffusion that is supposed to dominate plankton mixing [52], when $d_h < d_p$ is allowed. The other reason for choosing such parameter is that it is well-known new patterns, such as Turing patterns, can emerge in reaction-diffusion systems in which there is an imbalance between the diffusion coefficients d_p and d_h [23, 53]. Therefore, we set $\nu = d_h/d_p$, and investigated whether a spiral wave would break up into complex spatiotemporal chaos when the diffusion ratio was varied. Throughout this paper, we fix $d_p = 0.05$ and d_h is a control parameter.

In the following, we will show that the dynamic behavior of the spiral wave qualitatively change as the control parameter d_h increases from zero, i.e., the diffusion ratio ν increases from zero, to more than one. For large ν ($\nu > 1$), the outwardly rotating spiral wave is completely stable everywhere, and fills in the space when the proper parameters are chosen, as shown in Fig. 3(A). Figure 3(A) shows a series of snapshots of a well-developed single spiral wave formed spontaneously for the variable p in system (1). The spiral is initiated on a 600×600 grid by the cross-field protocol (the initial distribution chosen in the form of allocated "constant-gradient" perturbation of the co-existence steady state) and zero boundary conditions are employed for simulations in the two dimensions. From Fig. 3(A) we can see that the well-developed spiral waves are formed firstly by the evolution. Inside the domain, new waves emerge, but are evolved by the spiral wave growing from the center. The spiral wave can steadily grow and finally prevail over the whole domain (a movie illustrating the dynamical evolution for this case [54] [partly *movie_1*, *movie_2*, and *movie_3* for $d_h = 0.2$]). Fig. 3(B) shows that the spiral wave first break up far away from the core center and eventually relatively large spiral fragments are surrounded by a 'turbulent' bath remain. The size of the surviving part of the spiral does not shrink when d_h is further decreasing until finally d_h equals to 0, which is different from phenomenon that is observed previous in the two-dimensional space Belousov-Zhabotinsky and FitzHugn-Nagumo oscillatory system [30, 31, 55, 56, 57], in which the breakup gradually invaded the stable region near the core center, and finally the spiral wave broke up in the whole medium. Figure 3(C) is the time sequences (arbitrary units) of the variables p and h at an arbitrary spatial point within the spiral wave region, from which we can see that the spiral waves are caused by the accepted as "phase waves" with substantially group velocity, phase velocity and sinusoidal oscillation rather than the relaxational oscillation with large amplitude. This breakup scenario is similar to the breakup of rotating spiral waves observed in numerical simulation in chemical systems [30, 31, 55, 56, 57], and experiments in BZ systems [58, 59], which shows that spiral wave breakup in these systems was related to the Eckhaus instability and more important, the absolute instability.

The corresponding trajectories of the spiral core and the spiral arm (far away from the core center) at $y = 300$ are shown in Fig. 4, respectively. From Fig. 4, we can see that the spiral core is not completely fixed, but oscillates with a large amplitude. However, as d_h decreases to a critical value, an unstable modulation develops in

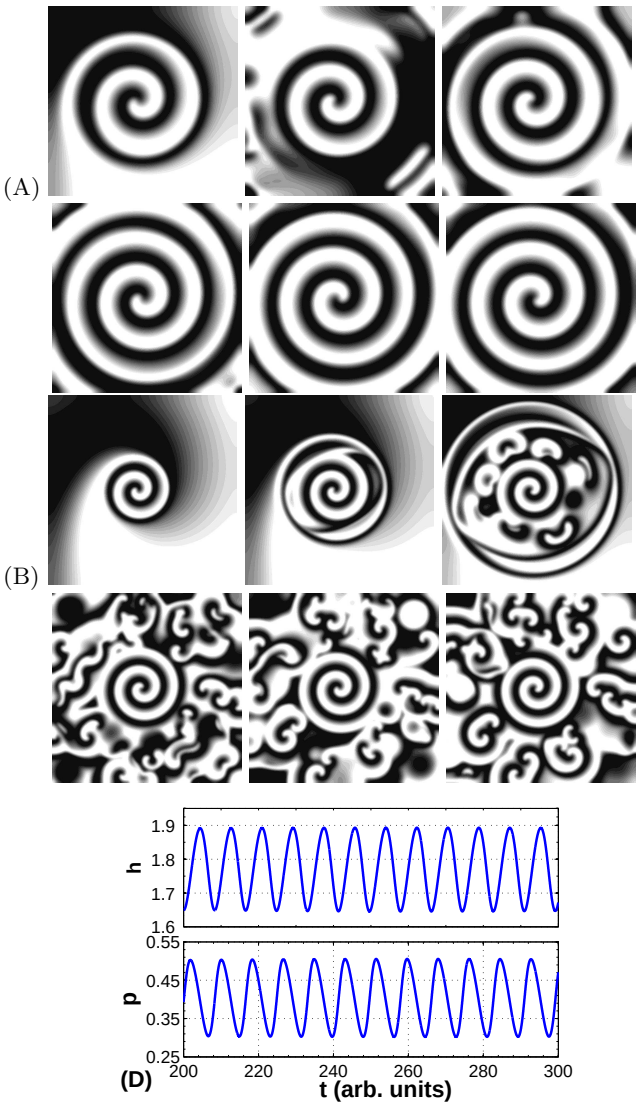

FIG. 3: Well developed spiral waves and some properties of them. The figures show simulations of the system (1) with $r = 5$, $a = 5$, $b = 5$, $m = 0.6$, $n = 0.4$, $d_p = 0.05$, and $f = 0.3$. (A) Well developed spiral waves shown at subsequent snapshot in time, $d_h = 0.2$. (B) Far-field breakup of the spiral waves shown at subsequent snapshot in time, $d_h = 0.002$. The white (black) areas correspond to maximum (minimum) values of p [Additional movie format available from Ref. [54]]. (C) Oscillations of the variable p and h at an arbitrary spatial point within the regular spiral wave region for both scenarios. Each figure is ran the long time until it spatial patterns are unchange.

regions which is far away from the spiral core (cf. the middle column of the Fig. 4). These oscillations eventually grow large enough to cause the spiral arm far away from the core to breakup into complex multiple spiral waves, while the core region remains stable (the corresponding movie can be viewed in the online supplemental in Ref. [54] [partly *movie_1* and *movie_2*, and for $d_h = 0.02$]). Figures 3(B) and 4(B) show the dynamic behavior for $d_h = 0.02$, i.e., $\nu = 0.4$. The regular trajectories far away from the core are now the same as the region of the spatial chaos (cf. the middle column of the Fig. 4). It is shown that an decrease in the diffusion ratio ν which leads to population oscillations of increasing amplitude (cf. the left column of the Fig. 4). In the tradition explain that the minimum value of the population density decreases and population extinction becomes more probable due to stochastic environmental perturbations. However, from the spatial evolution of system (1) (see Fig. 3), the temporal variations of the density of different sub-population can become asynchronous and the events of local extinction can be compensated due to re-colonization (or diffusion) from other sites.

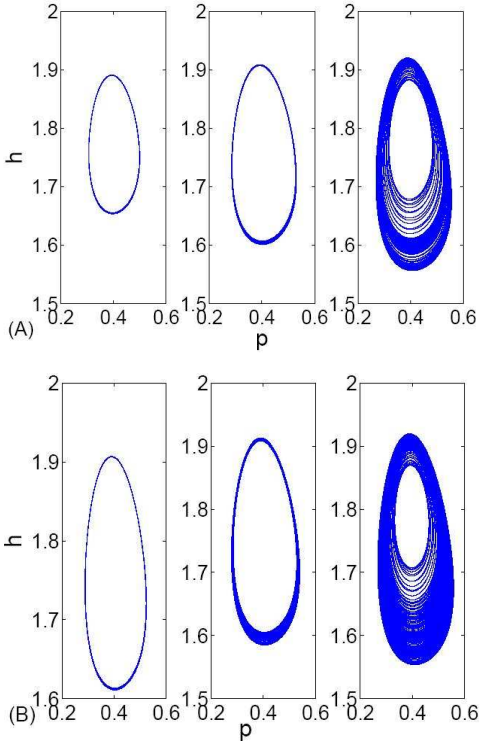

FIG. 4: The corresponding trajectories (from left to right) for locations $(300, 300)$, $(250, 300)$, and $(50, 300)$ respectively. The parameters in (A), and (B) were the same as these in Fig. 3(A) and (B), respectively.

Furthermore, it is well known that the basic arguments in spiral stability analysis can be carried out by reducing the system to one dimensional space [30, 31, 55, 56, 57]. Here we show some essential properties of the spiral breakup resulting from the numerical simulation. In the next section we will give the theoretical computation by using the eigenvalue spectra. In this model, it is worth noting that we do not neglect the oscillation of the dynamics in the core as shown in Fig. 4 due to the system exhibiting spatial periodic wave trains when the model is simulated in one-dimensional space. Breakup occurs first far away from the core (the source of waves). The spiral wave breaks towards the core until it gets to some

constant distance and then the surviving part of the spiral wave stays stable. These minimal stable wavelengths are called λ_{min}. So the one-parameter family may be described by a dispersion curve $\lambda(d_h)$ (see Fig. 5). The minimal stable wavelength λ_{min} of the spiral wave are shown in Fig. 5 coming from the simulation in two dimensional space. The results of Fig. 5 can be interpreted as follows: the minimal stable wavelengths decrease with respect to the decrease of d_h but eventually stay at a relative constant value, which is that the stable spiral waves are always existing for a larger region values of d_h. Space-time plots at different times are shown in Fig. 6 for two different d_h, i.e., different ν, which display the time evolution of the spiral wave along the cross section in the two-dimensional images of Fig. 3(A) and (B). As shown in Fig. 6(A) and (B) for $d_h = 0.2$ and $d_h = 0.02$ respectively, the waves far away from the core display unstable modulated perturbation due to convective instability [30, 31, 55, 56, 57], but this perturbation is gradually advected to the left and right sides, and finally disappears. The instability manifests itself to produce the wave train breakup several waves from the far-field, as shown in Figs. 6(B).

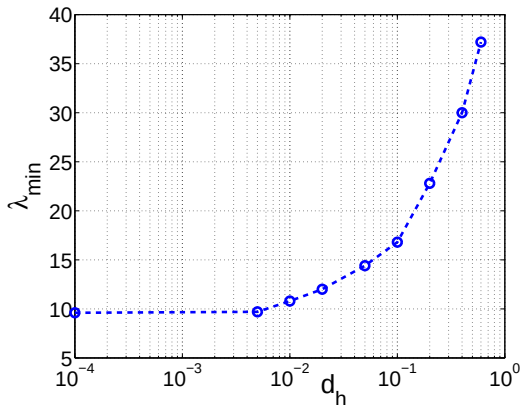

FIG. 5: Dependence of the wavelength λ_{min} on the parameter d_h for the system (1) with $r = 5.0$, $a = 5.0$, $b = 5.0$, $m = 0.6$, $d_p = 0.05$, and $n = 0.4$. Note the log scale for d_h.

IV. SPECTRA AND NONLINEAR BIFURCATION OF THE SPIRAL WAVE

In this section, we concentrate on the linear stability analysis of spiral wave by using the spectrum theory [56, 60, 61, 62, 63]. From the results in Refs. [56, 62] we know that the absolute spectrum must be computed numerically for any given reaction-diffusion systems. In practice, such computations only require discretization in one-dimensional space and compare with computing eigenvalues of the full stability problem on a large domain due to the spiral wave exhibitting traveling waves in the plane (see Fig. 6 about the space-time graphes). For spiral waves on the unbounded plane, the essential

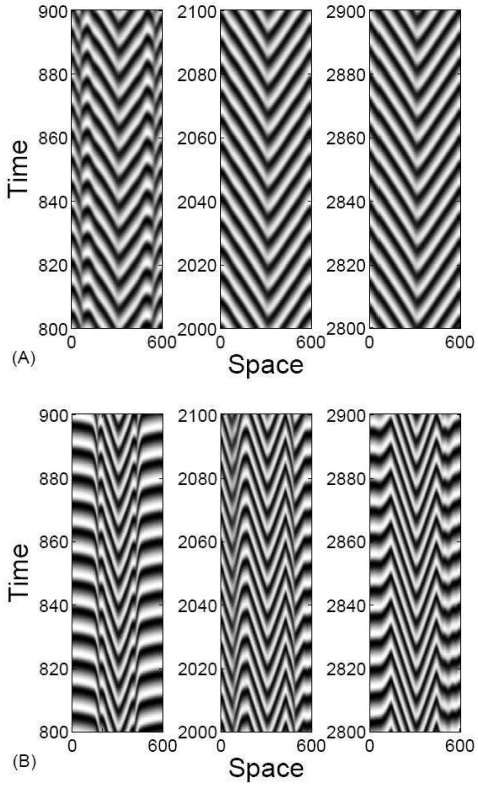

FIG. 6: Space-time plots of variable p for different time and d_h. The parameters in (A), and (B) are the same as those in Fig. 3(A) and (B), respectively.

spectrum is also required to compute, since it determined only by the far-field wave trains of the spiral. The linear stability spectrum consists of point eigenvalues and the essential spectrum that is a continuous spectrum for spiral waves.

For sake of simplicity, the Eqs. (1a) and (1b) can been written as following

$$\frac{\partial p}{\partial t} = d_p \nabla^2 p + g_1(p, h), \tag{3a}$$

$$\frac{\partial h}{\partial t} = d_h \nabla^2 h + g_2(p, h). \tag{3b}$$

Suppose that (p^*, h^*) are a solutions and refer to them as steady spirals of Eq. (3) that rotate rigidly with a constant angular velocity ω, and that are asymptotically periodic along rays in the plane. In a coratating coordinate frame, using the standardized analysis method for the spiral waves [62, 63], the Eq. (3) is given by

$$\frac{\partial p}{\partial t} = d_p \nabla^2_{\rho,\theta} p + \omega \frac{\partial p}{\partial \theta} + g_1(p^*, h^*), \tag{4a}$$

$$\frac{\partial h}{\partial t} = d_h \nabla^2_{\rho,\theta} h + \omega \frac{\partial h}{\partial \theta} + g_2(p^*, h^*), \tag{4b}$$

where (ρ,θ) denote polar coordinates, spirals waves are relative equilibria, then the statianry solutions $p^*(\rho,\theta)$ and $h^*(\rho,\theta)$ both are 2π-periodic functions with $\theta=\varphi-\omega t$. In Eqs. (4a) and (4b) the operator $\nabla^2_{\rho,\theta}$ denotes $\partial_{\rho\rho}+\frac{1}{\rho}\partial_\rho+\frac{1}{\rho^2}\partial_{\theta\theta}$.

A. Computation of spiral spectra

Next, we commpute the leading part of its linear stability spectrum for the system (4). Consider the linearized evolution equation in the rotating frame, the eigenvalue problem of Eqs. (4a) and (4b) associated with the planar spiral solutions $p^*(\rho,\theta)$ and $h^*(\rho,\theta)$ are given by

$$d_p\nabla^2_{\rho,\theta}p+\omega\frac{\partial p}{\partial\theta}+g_1^p(p^*,h^*)p+g_1^h(p^*,h^*)h=\lambda p, \quad (5a)$$

$$d_h\nabla^2_{\rho,\theta}h+\omega\frac{\partial h}{\partial\theta}+g_2^p(p^*,h^*)p+g_2^h(p^*,h^*)h=\lambda h, \quad (5b)$$

where g_1^p, $\cdots$, g_2^h denote the derivatives of the nonlinear functions and $g_1^p(p,h)=r(1-p)-rp-\frac{ah}{1+bp}+\frac{abph}{(1+bp)^2}$, $g_1^h(p,h)=-\frac{ap}{1+bp}$, $g_2^p(p,h)=\frac{ah}{1+bp}-\frac{abph}{(1+bp)^2}$, and $g_2^h(p,h)=\frac{ap}{1+bp}-m-\frac{2fnh}{n^2+h^2}+\frac{2fnh^3}{(n^2+h^2)^2}$. We shall ignore isolated eigenvalues that belong to the point spectrum, instabilities caused by point eigenvalues lead to meanderingor drifting waves, or to an unstable tip motionin in excitable media and oscillation media [56, 64, 65, 66]. This phenomenon is not shown in the present paper. Instead, we focus on the continuous spectrum that is responsible for the spiral wave breakup in the far field (see Fig. 3(b)). By the results in Ref. [62], it turns out that the boundary of the continuous spectrum depends only on the limiting equation for $\rho\to\infty$. Thus, we have that λ is the boundary of the continuous spectrum if, and only if the limiting equation

$$d_p\nabla^2_{\rho,\rho}p+\omega\frac{\partial p}{\partial\theta}+g_1^p(p^*,h^*)p+g_1^h(p^*,h^*)h=\lambda p, \quad (6a)$$

$$d_h\nabla^2_{\rho,\rho}h+\omega\frac{\partial h}{\partial\theta}+g_2^p(p^*,h^*)p+g_2^h(p^*,h^*)h=\lambda h, \quad (6b)$$

have solutions $p(\rho,\theta)$ and $h(\rho,\theta)$ for $(\rho,\theta)\in R^+\times[0,2\pi]$, which are bounded but does not decay as $\rho\to\infty$. Since spiral waves are rotating waves in the plane, the wave train solutions have the form as $u(t,x,y)=u(\rho,\varphi-\omega t)$ for an appropriate wave numbers k and temporal frequency ω, where we assume that u is 2π-periodic in its argument so that $u(\xi)=u(\xi+2\pi)$ for all ξ and $u=(p,h)^{\mathrm{T}}$. Spiral waves converge to wave trains $u(\rho,\varphi-\omega t)\to u_{wt}(k\rho+\varphi-\omega t)$ for $\rho\to\infty$, which are corresponding to asymptotically Archimedean in the two-dimensional space. Assume that $k\neq0$ and $\omega\neq0$, and in this case, we can pass from the theoretical frame ρ to the comoving frame $\xi=k\rho+\varphi-\omega t$ ($\xi\in\mathcal{R}$) in which the eigenvalue equation (6) becomes

$$d_pk^2\nabla^2_{\xi,\xi}p+\omega p_\xi+g_1^p(u_{wt}(\xi))p+g_1^h(u_{wt}(\xi))h=\lambda p, \quad (7a)$$

$$d_hk^2\nabla^2_{\xi,\xi}h+\omega h_\xi+g_2^p(u_{wt}(\xi))p+g_2^h(u_{wt}(\xi))h=\lambda h \quad (7b)$$

Indeed, any nontrivial solution $u(\xi)=(p(\xi),h(\xi))^{\mathrm{T}}$ corresponding to the linearization eigenvalue problem (7) give a solution $U(\rho,\cdot)$ of the eigenvalue problem for the temporal period map of (3) in the corotating frame via

$$U(\rho,\cdot)=e^{\lambda t}u(k\rho-\omega t),\qquad U(\rho,T)=e^{\lambda T}u(k\rho-2\pi). \quad (8)$$

We write the equations (7) as the first-order systems

$$\begin{aligned}\frac{dp}{d\rho}&=p_1,\\ \frac{dh}{d\rho}&=h_1,\\ \frac{dp_1}{d\rho}&=k^{-2}d_p^{-1}\big[\mu p-\omega p_1-g_1^p(u_{wt}(\xi))p-g_1^h(u_{wt}(\xi))h\big],\\ \frac{dh_1}{d\rho}&=k^{-2}d_h^{-1}\big[\mu h-\omega h_1-g_2^p(u_{wt}(\xi))p-g_2^h(u_{wt}(\xi))h\big],\end{aligned} \quad (9)$$

in the radial variable ρ. Then the spatial eigenvalues or spatial Floquet exponents are determined as the roots of the Wronskian

$$\mathcal{A}(\lambda,k):=\begin{pmatrix}0&0&1&0\\0&0&0&1\\ \frac{1}{k^2d_p}(\lambda-g_1^p(u_{wt}(\xi)))&-\frac{1}{k^2d_p}g_1^h(u_{wt}(\xi))&-\frac{1}{k^2d_p}\omega&-\\ -\frac{1}{k^2d_h}g_2^p(u_{wt}(\xi))&\frac{1}{k^2d_h}(\lambda-g_2^h(u_{wt}(\xi)))&0&\end{pmatrix} \quad (10)$$

where $k\in\mathcal{R}$. The function $U(\rho,\cdot)=e^{\lambda t}e^{\mathrm{i}k\rho}u_0(k\rho-\omega t)$ satisfies the equation (3) when the spatial and temporal exponents $\mathrm{i}k$ and λ satisfy the complex dispersion relation $\det(\mathcal{A}(\lambda,k)-\mathrm{i}k)=0$ for $\lambda\in\mathcal{C}$. We call the $\mathrm{i}k$ in spectrum of $A(\lambda,k)$ as spatial eigenvalues or spatial Floquet exponents.

The stability of the spiral waves state (p^*,h^*) on the plane is determined by the essential spectrum given by

$$\Sigma_{ess}=\{\lambda\in\mathcal{C};\det(\mathcal{A}(\lambda,k)-\mathrm{i}k)=0\text{ for some }k\in\mathcal{R}\}. \quad (11)$$

Now, we compute the continuous spectrum with the equation (9) that are parameterized by the wave number k. For each λ, there are infinitely many stable and unstable spatial eigenvalues. We plot λ in the complex plane associated spatial spectrum, see Fig. 7. By the explaination of Sandstede *et al* [60], one would know that if the real part of the essentail spectra is positive, then the associated eigenmodes grow exponentially toward the boundary, i.e., they correspond to a far-field instability. Note that we find the essentail spectra are not sensitive to temporal frequency, ω.

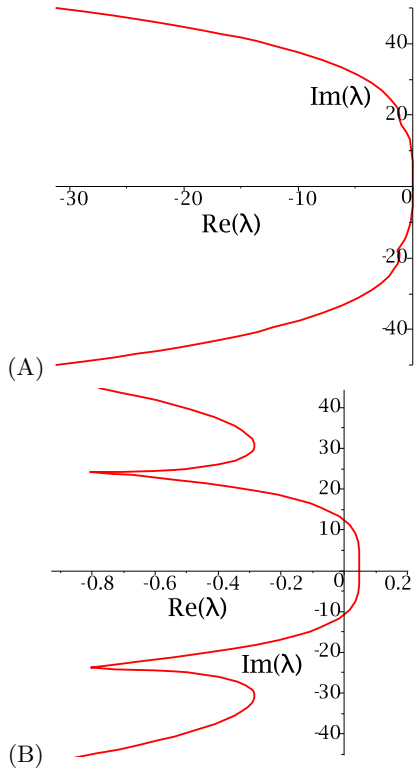

FIG. 7: The essentail spectra of wave trains are obtained by using the algorithms outlined in Refs. [60, 61]. The parameters of (A) and (B) are corresponding to the values used in the simulations of Fig. 3(A) and (B).

B. Existence and properties of wave trains

Suppose that a reaction-diffusion system on the one-dimensional space such that the variables equal to a homogeneous stationary solution. If the homogeneous steady-state destabilizes, then its linearization accommodates waves of the form $e^{\mathrm{i}(kx-\omega t)}$ for certain values k and ω. Typically, near the transition to instability, small spatially periodic travelling waves arise for any wave number close to k_c, which is the critical wavenumber. Their wave speed is approximately equal to $\frac{\omega_c}{k_c}$, where ω_c is corresponding to k_c. In present paper, we focus exclusively on the situation where $\omega_c = 0$ and $k_c \neq 0$. The bifurcation with $\omega_c = 0$ and $k_c \neq 0$ is known as the Turing bifurcation, and the bifurcating spatially periodic steady patterns are often referred to as Turing patterns. Another class of moved patterns will appear when the instabilities modulated by Hopf-Turing bifurcation, which is resemble a travelling waves. Moreover, the common feature of the spiral waves in one-dimensional space mentioned above is the presence of wave trains which are spatially periodic travelling waves of the form $p_{wt}(kx - \omega t; k)$ and $h_{wt}(kx - \omega t; k)$, where $p_{wt}(\phi; k)$ and $h_{wt}(\phi; k)$ are 2π-periodic about ϕ. Typically, the spatial wavenumber k and the temporal frequency ω are related via the nonlinear dispersion relation $\omega = \omega(k)$ so that the phase velocity is given by

$$c_p = \frac{\omega}{k}. \tag{12}$$

A second quantity related to the nonlinear dispersion relation is the group velocity, $c_g = \frac{d\omega}{dk}$, of the wave train which also play a central role in the spiral waves. The group velocity c_g gives the speed of propagation of small localized wave-package perturbations of the wave train [67]. Here, we are only concerned the existence of travelling wave solution. In fact, the spiral waves move at a constant speed outward from the core (see Fig. 6), so that they have the mathematical form $p(x,t) = P(z)$, and $h(x,t) = H(z)$ where $z = x - c_p t$. Substituting these solution forms into Eq. (3) gives the ODEs

$$d_p \frac{d^2P}{dz^2} + c_p \frac{dP}{dz} + g_1(P,H) = 0, \tag{13a}$$

$$h_p \frac{d^2H}{dz^2} + c_p \frac{dH}{dz} + g_2(P,H) = 0. \tag{13b}$$

Here, we investigate numerically the existence, speed and wavelength of travelling wave patterns. Our approach is to use the bifurcation package Matcont 2.4 [68] to study the pattern ODEs (13). To do this, the most natural bifurcation parameters are the wave speed c_p and f, but they give no information about the stability of travelling wave as solutions of the model PDEs (3).

Our starting point is the homogeneous steady state of Eq. (13) with in the domain III of Fig. 2. The typical bifurcation diagrams are illustrated in Fig. 8, which shows that steady spatially peroidic travelling waves exist for the larger values of the speed c_p, but it is unstable for small values of c_p. The changes in stability occur via Hopf bifurcation, from which a branch of periodic orbits emanate. Note that here we use the terms "stable" and "unstable" as referring to the ODEs system (13) rather than the model PDEs. Fig. 8(B) illustrates the maximun stable wavelength against the bifucation parameter, speed c_p, and the small amplitudes have very long wavelength. It is known that $c_p = \frac{\omega}{k}$, hence the tavelling wave solution exist when the $c_p \neq 0$, i.e., $k \neq 0, \omega \neq 0$. Using Matcont 2.4 package, it is possible to track the locus of the Hopf bifurcation points and the Limit point (fold) bifurcation in a parameter plane, and a typical example of this for the c_p-f and c_p-d_h plane are illustrated in Fig. 9. The travelling wave solutions exist for values of c_p and f lying in left of Hopf bifurcation locus (see Fig. 9(A)). The same structure about the c_p-d_h plane is shown in Fig. 9(B). These reuslts confirm our previous analysis coming from the algebra computation (see Fig. 2) and the numerical results (see Fig. 6).

V. CONCLUSIONS AND DISCUSSION

We have investigated a spatially extended plankton ecological system within two-dimensional space and

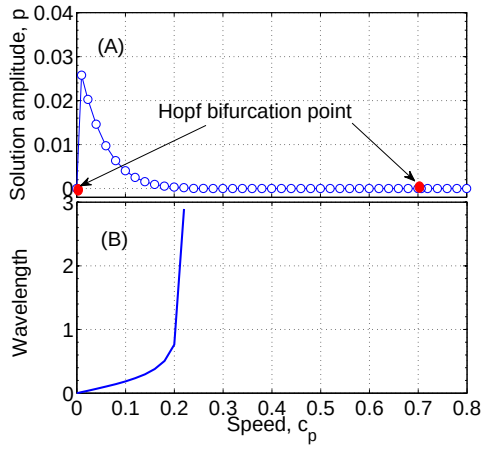

FIG. 8: Typical bifurcation diagrams for the pattern ODEs (13). (A) The spatially periodic travelling waves of system (3) is existence. The changes in stability occur via Hopf bifurcation, from which a branch of periodic orbits emanate. Thus unstable travelling waves appear. (B) Maximum stable wavelength along the bifurcation parameterc_p, i.e., $k \neq 0, \omega \neq 0$. The parameter values in (A) and (B) are the same as Fig. 3(A).

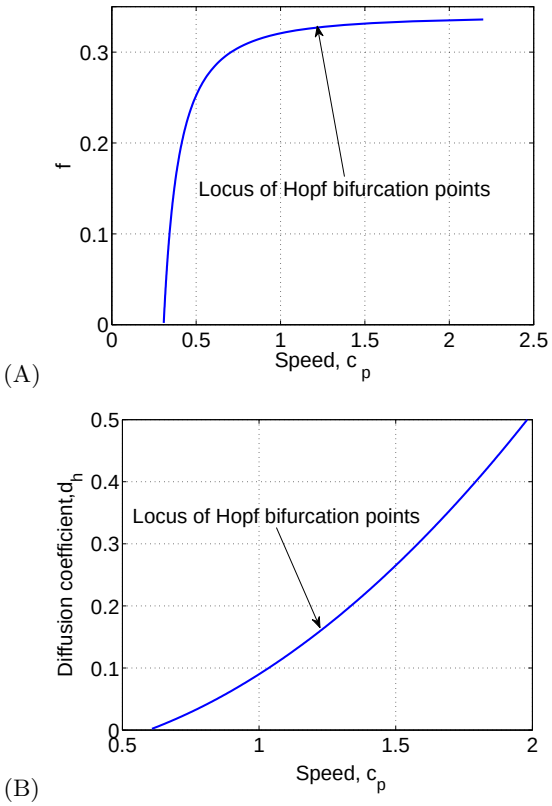

FIG. 9: An illustration of the variations in parameter space of the pattern ODEs (13). We plot the loci of Hopf bifurcation points. (A) $f - c_p$ planes; (B) $d_h - c_p$ planes. The parameter values in (A) and (B) are the same as Fig. 3(A).

found that its spatial patterns exhibit spiral waves dynamics and spatial chaos patterns. Specially, the scenario of the spatiotemporal chaos patterns arising from the far-field breakup is observed. Our research is based on numerical analysis of a kinematic mimicking the diffusion in the dynamics of marine organisms, coupled to a two component plankton model on the level of the community. By increasing (decreasing) the diffusion ratio of the two variables, the spiral arm first broke up into a turbulence-like state far away from the core center, but which do not invade the whole space. From the previous studies in the Belousov-Zhabotinsky reaction, we know the reason causing this phenomenon can be illuminated theoretically by the M. Bär and L. Brusch [30, 31], as well as by using the spectrum theory that poses by B. Sandstede, A. Scheel *et al* [56, 60, 61, 69]. The far-field breakup can be verified in field observation and is useful to understand the population dynamics of oceanic ecological systems. Such as that under certain conditions the interplay between wake (or ocean) structures and biological growth leads to plankton blooms inside mesoscale hydrodynamic vortices that act as incubators of primary production. From Fig. 3 and corresponding the movies, we see that spatial peridic bloom appear in the phytoplankton populations, and the details of spatial evolution of the distribution of the phytoplankton population during one bloom cycle, respectively.

In Ref. [70], the authors study the optimal control of the model (1) from the spatiotemporal chaos to spiral waves by the parameters for fish predation treated as a multiplicative control variable. Spatial order emerges in a range of spatial models of multispecies interactions. Unsurprisingly, spatial models of multispecies systems often manifests very different behaviors from their mean-field counterparts. Two important general features of spatial models of multispecies systems are that they allow the possibility of global persistence in spite of local extinctions and so are usually more stable than their mean-field equivalents, and have a tendency to self-organzie spatially or regular spatiotemporal patterns [70, 71]. The spatial structures produces nonrandom spatial patterns such as spiral waves and spatiotemporal chaos at scales much larger than the scale of interaction among individuals level. These structures are not explicitly coded but emerge from local interaction among individuals and local diffusion.

As we know that plankton plays an important role in the marine ecosystem and the climate, because of their participation in the global carbon and nitrogen cycle at the base of the food chain [72]. From the review [73], a recently developed ecosystem model incorporates different phytoplankton functional groups and their competition for light and multiple nutrients. Simulations of these models at specific sites to explore future scenarios suggest that global environmental change, including global-warming-induced changes, will alter phytoplankton community structure and hence alter global biogeochemical cycles [74]. The coupling of spatial ecosystem model to

global climate raises again a series of open questions on the complexity of model and relevant spatial scales. So the study of spatial model with large-scale is more important in the ecological system. Basing on numerical simulation on the spatial model, we can draft that the oceanic ecological systems show permanent spiral waves and spatiotemporal chaos in large-scale over a range of parameter values d_h, which indicates that periodically sustained plankton blooms in the local area. As with all areas of evolutionary biology, theoretical development advances more quickly than does empiraical evidence. The most powerful empirical approach is to conduct experiments in which the spatial pattern can be measured directly, but this is difficulties in the design. However, we can indirectly measured these phenomenona by the simulation and compared with the satellite pictures. For example, the spatiotemporal chaos patterns agree with the perspective observation of the Fig. 3 in Ref. [73]. Also, some satellite imageries [http://oceancolor.gsfc.nasa.gov] have displayed spiral patterns that represent the phytoplankton [the chlorophyll] biomass and thus demonstrated that plankton patterns in the ocean occur on much broader scales and therefore mechanisms thought diffusion should be considered.

Acknowledgments

This work is supported by the National Natural Science Foundation of China under Grant No. 10471040 and the Natural Science Foundation of Shan'xi Province Grant No. 2006011009.

[1] R. E. Amritkar and Govindan Rangarajan. Spatially synchronous extinction of species under external forcing. *Phys. Rev. Lett.*, 96(25):258102, 2006.

[2] Andrzej Pekalski and Michel Droz. Self-organized packs selection in predator-prey ecosystems. *Phys. Rev. E*, 73(2):021913, 2006.

[3] Y.-Y. H. Sayama, M. A. M. de Aguiar, and M. Baranger. Interplay between turing pattern formation and domain coarsening in spatially extended population models. *FORMA*, 18:19, 2003.

[4] E. Gilad, J. von Hardenberg, A. Provenzale, M. Shachak, and E. Meron. Ecosystem engineers: From pattern formation to habitat creation. *Phys. Rev. Lett.*, 93(9):098105, 2004.

[5] Mark J Washenberger, Mauro Mobilia, and Uwe C Täuber. Influence of local carrying capacity restrictions on stochastic predator–prey models. *J. Phys.: Cond. Matt.*, 19(6), 2007.

[6] Mauro Mobilia, Ivan Georgiev, and Uwe Täuber. Phase transitions and spatio-temporal fluctuations in stochastic lattice lotkacvolterra models. *J. Stat. Phys.*, 128(1):447–483, 2007.

[7] Bernd Blasius, Amit Huppert, and Lewi Stone. Complex dynamics and phase synchronization in spatially extended ecological systems. *Nature*, 399(6734):354–359, 1999.

[8] J. von Hardenberg, E. Meron, M. Shachak, and Y. Zarmi. Diversity of vegetation patterns and desertification. *Phys. Rev. Lett.*, 87(19):198101, 2001.

[9] A. Provata and G. A. Tsekouras. Spontaneous formation of dynamical patterns with fractal fronts in the cyclic lattice lotka-volterra model. *Phys. Rev. E*, 67(5):056602, 2003.

[10] Alexander B. Medvinsky, Irene A. Tikhonova, Rubin R. Aliev, Bai-Lian Li, Zhen-Shan Lin, and Horst Malchow. Patchy environment as a factor of complex plankton dynamics. *Phys. Rev. E*, 64(2):021915, 2001.

[11] Alexander B. Medvinsky, Sergei V. Petrovskii, Irene A. Tikhonova, Horst Malchow, and Bai-Lian Li. Spatiotemporal complexity of plankton and fish dynamics. *SIAM Review*, 44:311–370, 2002.

[12] W. S. C. Gurney, A. R. Veitch, I. Cruickshank, and G. McGeachin. circles and spirals: population persistence in a spatially explicit predatorcprey model. *Ecology*, 79(7):2516–2530, 1998.

[13] J. D. Murray. *Mathematical biology.* Interdisciplinary applied mathematics. Springer, New York, 3rd edition, 2002.

[14] Sergei Petrovskii, Bai-Lian Li, and Horst Malchow. Transition to spatiotemporal chaos can resolve the paradox of enrichment. *Ecological Complexity*, 1:37–47, 2004.

[15] Laurence Armi, Dave Hebert, Neil Oakey, James Price, Philip L. Richardson, Thomas Rossby, and Barry Ruddick. The history and decay of a mediterranean salt lens. *Nature*, 333(6174):649–651, 1988.

[16] Esa Ranta, Veijo Kaitala, and Per Lundberg. The Spatial Dimension in Population Fluctuations. *Science*, 278(5343):1621–1623, 1997.

[17] L S Luckinbill. The effects of space and enrichment on a predator-prey system. *Ecology*, 55:1142–1147, 1974.

[18] M Holyoak. Effects of nurient enrichment on predator-prey metapopulation dynamics. *J Anim. Ecol.*, 69:985–997, 2000.

[19] Vincent A.A. Jansen. Regulation of predator-prey systems through spatial interactions: a possible solution to the paradox of enrichment. *Oikos*, 74:384390, 1995.

[20] Vincent A.A. Jansen and Alun L. Lloyd. Local stability analysis of spatially homogeneous solutions of multipatch systems. *J. Math. Biol.*, 41:232252, 2000.

[21] Vincent A.A. Jansen. The dynamics of two diffusively coupled predatorprey populations. *Theor. Popul. Biol.*, 59:119131, 2001.

[22] J. C. Allen, W. M. Schaffer, and D. Rosko. Chaos reduces species extinction by amplifying local population noise. *Nature*, 364:229232, 1993.

[23] M. C. Cross and P. C. Hohenberg. Pattern formation outside of equilibrium. *Rev. Mod. Phys.*, 65(3):851, 1993.

[24] Kyoung J. Lee, Raymond E. Goldstein, and Edward C. Cox. Resetting wave forms in dictyostelium territories. *Phys. Rev. Lett.*, 87(6):068101, 2001.

[25] Satoshi Sawai, Peter A. Thomason, and Edward C. Cox. An autoregulatory circuit for long-range self-organization

in dictyostelium cell populations. *Nature*, 433(7023):323–326, 2005.

[26] Arthur T. Winfree. Varieties of spiral wave behavior: An experimentalist's approach to the theory of excitable media. *Chaos*, 1(3):303–334, 1991.

[27] V. N. Biktashev, J. Brindley, A. V. Holden, and M. A. Tsyganov. Pursuit-evasion predator-prey waves in two spatial dimensions. *Chaos*, 14(4):988–994, 2004.

[28] M Garvie. Finite-difference schemes for reaction-diffusion equation modeling predato-prey interactions in matlab. *Bull. Math. Biol.*, 69:931–956, 2007.

[29] Marcus R. Garvie and Catalin Trenchea. Optimal control of a nutrient-phytoplankton-zooplankton-fish system. *SIAM J. Contr. and Opti.*, 46(3):775–791, 2007.

[30] Markus Bär and Lutz Brusch. Breakup of spiral waves caused by radial dynamics: Eckhaus and finite wavenumber instabilities. *New Journal of Physics*, 6:5, 2004.

[31] Markus Bär and Michal Or-Guil. Alternative scenarios of spiral breakup in a reaction-diffusion model with excitable and oscillatory dynamics. *Phys. Rev. Lett.*, 82(6):1160–1163, 1999.

[32] Craig R Johnson and Maarten C Boerlijst. Selection at the level of the community: the importance of spatial structure. *Trends Ecol. and Evol.*, 17:83–90, 2002.

[33] M Pascual. Diffusion-induced chaos in a spatial predatorprey system. *Proc. R. Soc. Lond. B*, 251:17, 1993.

[34] J. A. Sherratt, B. T. Eagan, and M. A. Lewis. Oscillations and chaos behind predatorprey invasion: mathematical artifact or ecological reality? *Phil. Trans. R. Soc. Lond. B*, 352:2138, 1997.

[35] S. V. Petrovskii and H. Malchow. Wave of chaos: new mechanism of pattern formation in spatio-temporal population dynamics. *Theor. Popul. Biol.*, 59:157174, 2001.

[36] J. A. Sherratt. Periodic travelling waves in cyclic predatorprey systems. *Ecol. Lett.*, 4:3037, 2001.

[37] N. J. Savill and P. Hogeweg. Spatially induced speciation prevents extinction: the evolution of dispersal distance in oscillatory predator-prey models. *Proc. R. Soc. Lond. B*, 265(1390):25–32, 1998.

[38] E. R. Abraham. The generation of plankton patchiness by turbulent stirring. *Nature*, 391:577–580, 1998.

[39] Carol L. Folt and Carolyn W. Burns. Biological drivers of zooplankton patchiness. *Nature*, 14:300–305, 1999.

[40] M Scheffer. Should we expect strange attractors behind plankton dynamics and if so, should we bother? *J. Plankton Res.*, 13:1291–1305, 1991.

[41] I. Hanski, P. Turchin, E. Korplmakl, and H. Henttonen. Population oscillations of boreal rodents: regulation by mustelid predators leads to chaos. *Nature*, 364:232235, 1993.

[42] S. Ellner and P. Turchin. Chaos in a noisy world: new methods and evidence from time-series analysis. *Am. Nat.*, 145:343375, 1995.

[43] B. Dennis, R. A. Desharnais, J. M. Cushing, S. M. Henson, and R. F. Costantino. Estimating chaos and complex dynamics in an insect population. *Ecol. Monogr.*, 71:277303, 2001.

[44] M Scheffer. Fish and nutrients interplay determines algal biomass: A minimal model. *Oikos*, 62:271–282, 1991.

[45] H. Malchow. Spatio-temporal pattern formation in nonlinear non-equilibrium plankton dynamics. *Procc. R. Soc. Lond. B*, 251:103, 1993.

[46] M. Pascual. Diffusion-induced chaos in a spatial predator-prey system. *Procc. R. Soc. Lond. B*, 251:1–7, 1993.

[47] Arnd Scheel. Radialy symmetric patterns of reaction-diffusion systems. *Mem. Amer. Math. Soc.*, 165:86, 2003.

[48] R A Satnoianu, M Menzinger, and P K Maini. Turing instabilities in general system. *J. Math. Biol.*, 41:493–512, 2000.

[49] Quan-Xing Liu, Bai-Lian Li, and Zhen Jin. Resonant patterns and frequency-locked induced by additive noise and periodically forced in phytoplankton-zooplankton system, 2007.

[50] Sven Erik Jørgensen and G. Bendoricchio. *Fundamentals of ecological modelling*. Developments in environmental modelling; 21. Elsevier, Amsterdam; New York, 3rd edition, 2001.

[51] Akira Okubo. *Diffusion and ecological problems: mathematical models*. Biomathematics; v. 10. Springer-Verlag, Berlin; New York, 1980.

[52] George Sugihara and Robert M. May. Nonlinear forecasting as a way of distinguishing chaos from measurement error in time series. *Nature*, 344(6268):734–741, 1990.

[53] A. M. Turing. The chemical basis of morphogenesis. *Philosophical Transactions of the Royal Society of London. Series B, Biological Sciences*, 237(641):37–72, 1952.

[54]

[55] Fagen Xie, Dongzhu Xie, and James N. Weiss. Inwardly rotating spiral wave breakup in oscillatory reaction-diffusion media. *Phys. Rev. E*, 74(2):026107, 2006.

[56] Björn Sandstede and Arnd Scheel. Absolute versus convective instability of spiral waves. *Phys. Rev. E*, 62(6):7708–7714, 2000.

[57] S. M. Tobias and E. Knobloch. Breakup of spiral waves into chemical turbulence. *Phys. Rev. Lett.*, 80(21):4811–4814, 1998.

[58] Q. Ouyang and J. M. Flesselles. Transition from spirals to defect turbulence driven by a convective instability. *Nature*, 379(6561):143–146, 1996.

[59] Qi Ouyang, H. L. Swinney, and G. Li. Transition from spirals to defect-mediated turbulence driven by a doppler instability. *Phys. Rev. Lett.*, 84(5):1047–1050, 2000.

[60] Björn Sandstede and Arnd Scheel. Curvature effects on spiral spectra: Generation of point eigenvalues near branch points. *Phys. Rev. E*, 73:016217, 2006.

[61] Jens D.M. Rademacher, Björn Dandstede, and Arnd Scheel. Computing absolute and essential spectra using continuation. *Physics D*, 229:166–183, 2007.

[62] P. Wheeler and D. Barkley. Computation of Spiral Spectra. *SIAM J Appl. Dynam. Syst.*, 2006.

[63] Björn Sandstede and Arnd Scheel. Absolute and convective instabilities of waves on unbounded and large bound domians. *Physics D*, 145:233–277, 2000.

[64] Dwight Barkley. Linear stability analysis of rotating spiral waves in excitable media. *Phys. Rev. Lett.*, 68(13):2090–2093, 1992.

[65] Dwight Barkley. Euclidean symmetry and the dynamics of rotating spiral waves. *Phys. Rev. Lett.*, 72(1):164–167, 1994.

[66] Igor Aranson, Lorenz Kramer, and Andreas Weber. Core instability and spatiotemporal intermittency of spiral waves in oscillatory media. *Phys. Rev. Lett.*, 72(15):2316–2319, 1994.

[67] Björn Sandstede and Arnd Scheel. Defects in oscillatory media: Toward a classification. *SIAM J. Appl. Dynam. Syst.*, 3(1):1–68, 2004.

[68] A Dhooge, W Govaerts, Yu A Kuznetsov, W Mestrom,

A M Riet, and B Sautois. *Matcont and Cl-Matcont: Continuation toolboxes in Matlab*. Utrecht University, The Netherlands, 2006.

[69] Paul Wheeler and Dwight Barkley. Computation of spiral spectra. *SIAM J. Appl. Dynam. Syst.*, 5:157–177, 2006.

[70] Maarten C. Boerlijst. *The Geometry of Ecological Interactions: Simplifying Spatial Complexity*, chapter Spirals and spots: Novel Evolutionary Phenomena through spatial self-structuring, pages 171–182. Cambridge University Press, 2000.

[71] Ulf Dieckmann, Richard Law, and Johan A J Metz. *The Geometry of Ecological Interactions: Simplifying Spatial Complexity*. Cambridge University Press, 2000.

[72] J. Duinker and G. Wefer. Das co2-problem und die rolle des ozeans. *Naturwissenschaften*, 81(6):237–242, 1994.

[73] M. Pascual. Computational ecology: From the complex to the simple and back. *Plos Comput. Biol.*, 1(2):101–105, 2005.

[74] E. Litchman, C. A. Klausmeier, J. R. Miller, O. M. Schofield, and P. G. Falkowski. Multi-nutrient, multi-group model of present and future oceanic phytoplankton communities. *Biogeosciences*, 3(4):585–606, 2006.